Determination of the dynamic tensile response and dissipated fracture energy of concrete with a cohesive element model

F. Gatuingt, Léonardo Snozzi, Jean-François Molinari

Determination of the dynamic tensile response and dissipated fracture energy of concrete with a cohesive element model

Numerical Modeling
Strategies for Sustainable Concrete Structures
Aix en Provence, France
May 29-June 1, 2012

F. Gatuingt[1], L. Snozzi[2], J.F. Molinari[2]

[1] *LMT-Cachan (ENS Cachan/CNRS/Université Paris 6/PRES UniverSud Paris), France*
fabrice.gatuingt@ens-cachan.fr
[2] *LSMS, School of Architecture, Civil and Environmental Engineering (ENAC),*
ÉCOLE POLYTECHNIQUE FÉDÉRALE DE LAUSANNE (EPFL), Switzerland

1 Introduction

Modelling of concrete structures subjected to dynamic loading such as explosions, impacts and perforations is very demanding, both from the point of view of computer codes and from the point of view of material modelling. Several macroscopic models for concrete have been developed [1, 2, 3, 4, 5, 6, 7, 8, 9, 10] to perform non-linear numerical analysis of such problems. In these models a rate effect in tension has often been introduced to represent the experimental data for loading strain rates exceeding 1 /s [11, 12]. The influence of the internal microstructure of concrete and the mechanisms that lead to different crack patterns when varying the loading rate, remain open questions. In order to give some answers to these questions, concrete has to be considered as a heterogeneous material where the nature of the heterogeneity depends essentially on the scale of observation. If one takes the scale of sand's grain, concrete can be considered as a biphasic material made of aggregates of different sizes randomly distributed in a mortar matrix. Thus, the failure of a concrete sample in tension is related to processes that take place at the so-called mesoscale. In order to investigate the role of the meso-structure on the dynamic tensile response of concrete, one can use a numerical approach. This is achieved in this paper using a 2D finite element mesoscopic description of concrete (aggregates + matrix) with cohesive capability. This method has proven its efficiency on numerical simulations of fracture of brittle materials [13] and has been extended to concrete like materials [14].

2 Meso-scale model

Concrete is an heterogeneous material made of various components, which are present in different proportions. This produces a quasi-brittle material, whose mechanical behavior is defined by the wide range of the ingredients in the mixture. Since every component has an influence according to its characteristic length, considering concrete at a meso-scale level of observation allow to represent it as a biphasic material: aggregates embedded in a mortar paste matrix. Meso-scale continuum models have been tested by several authors [15, 16, 17, 18]. From those works it results that the meso-scale level of material observation is suitable to capture the main characteristics of the overall mechanical behavior of concrete: micro-cracking, fracture initiation and propagation, coalescence and localization. Moreover the constitutive equations might be relaxed when comparing with a macro-scale formulation and thus the number of parameters may be reduced.

In our model only medium and large aggregates are represented explicitly. Besides those two components the interfaces between the two phases, called interfacial transition zone (ITZ), are represented by dynamically inserted elements with the presented cohesive-frictional capability. In order to study the specific effect of the meso-structure on the dynamic tensile response, no random fields have been introduced on the properties. A finite element approach with cohesive capability is then used to simulate the cracks opening and propagation.

2.1 Meso-structure modelisation

Real concrete is based on randomly distributed aggregates in a cement paste matrix. In our description, we chose to describe explicitly only the aggregates with a diameter larger than 4 mm and smaller than 25 mm with six classes to capture roughly the aggregates size distribution. The smallest aggregates are then taken into account in the homogeneous matrix of mortar. The size of the specimens generated is 100×100 mm^2. As in [19], knowing the aggregate size distribution, the number of perfect circular (in 2D) aggregates of each class can be calculated. To avoid an artificial increase of the volume matrix due to the boundary effect, the heterogeneities are placed in a larger sample with a final cut of all parts outside of the concrete specimen. Figure 1 shows different images of the meso-structures obtained using this method with the same aggregate size distribution.

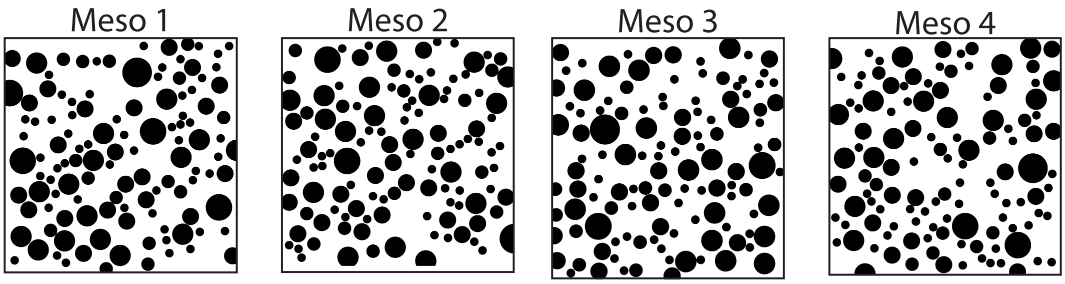

Figure 1: Different images of the meso-structures generated with the same aggregates size distribution.

A 2D finite element mesh is then generated from the meso-structure images using the PPM2OOF [20] public domain software created at the National Institute of Standards and Technology (NIST). Notice that this mesh generation is possible since the cohesive element methodology here does not require an a priori definition of the possible fracture planes [21, 15, 16, 22, 23, 18].

2.2 The cohesive element method

A well-known method to model the onset of fracture is to having recourse to cohesive zone modeling, which has been introduced by Dugdale [24] and Barenblatt [25] in the 1960's. This method describes fracture as a separation process by relating the displacement jump, which occurs at the crack tip, with tractions. The debonding is assumed to be confined in a small region of material called the cohesive zone, which represents the region where atomistic separation occurs. Within the computational framework this region is represented by interface elements with zero thickness. While damage is concentrated in these elements, the surrounding bulk material behaves linear elastically.

In our case the crack path is not known *a priori* and all lines in the mesh are considered as a potential crack path. During the simulation, the stress on the interface between two adjacent continuum elements is computed and compared to the fracture criterion at the end of every time step. The interfacial stress, σ, is calculated averaging stresses of the adjacent Gauss points of the two continuum elements. If the inter-element stress exceeds the critical stress value, the nodes located at the inter-element boundary are doubled, the two elements are topologically disconnected and a cohesive element is inserted (see Figure 2). After the nodal disconnection, the interfacial stress starts being controlled by the traction separation law implemented in the cohesive element (Figure 2).

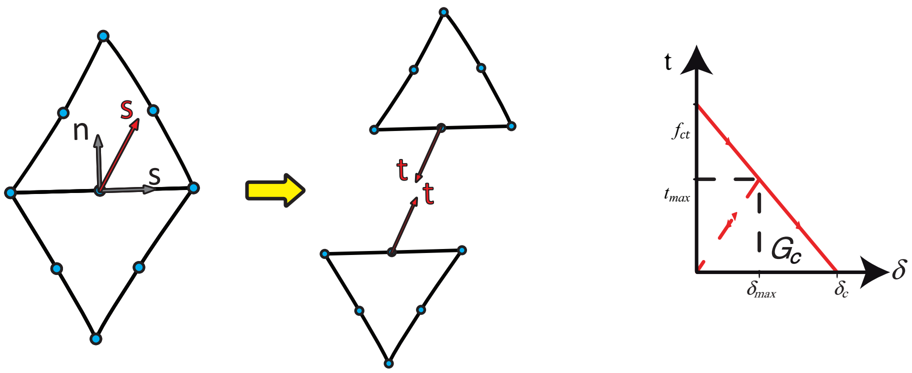

Figure 2: Schematics of the nodal disconnection between two continuum elements in which the interfacial stress has exceeded the critical stress and the traction/separation law

where t is the effective cohesive traction, f_{ct} represents the local material strength and δ_c represents the effective relative displacement beyond which complete decohesion occurs. Note that the definition of f_{ct} and δ_c implicitly establish the existence of an effective fracture energy G_c, which corresponds to the area under the curve of Figure 2:

$$G_c = \frac{1}{2} f_{ct} \delta_c \tag{1}$$

Partially damaged cohesive elements have dissipated an energy $W < G_c$. As the present work is focused on tensile uniaxial loading, the fracture energy of the different phases of our concrete is identified to the experimental one for Mode I, i.e. $G_c = G_c^I$.

3 Numerical simulation of direct tensile test in dynamics

3.1 Initial and boundary conditions

The specimen is loaded under displacement control with an imposed strain rate $\dot{\varepsilon}$. To avoid stress wave propagation and an early fracture near the boundaries [26], all the nodes of the finite element mesh are prescribed an initial velocity in accordance to their vertical position y as illustrated in Figure 3:

$$V_y(y) = \frac{2V_0}{h} y \tag{2}$$

To obtain the stress-strain curves, we define the macroscopic stress as the boundary reaction force F_y divided by the initial width of the specimen and the macroscopic strain as the displacement U_y of the boundary divided by the initial height h of the specimen.

3.2 Material parameters

As shown in section 2 our numerical model is based on three phases: the mortar paste, the aggregates and an ITZ. For these phases we have to identify the elastic and rupture parameters of equation 2.2. We used the parameters given in Table 1.

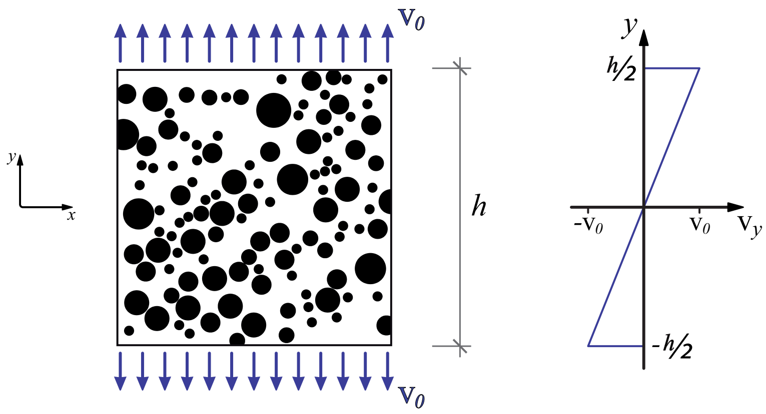

Figure 3: Velocity initial condition

Table 1: Material properties used in the simulations

	Aggregate	Mortar paste	ITZ
Density – ρ (kg/m^3)	2700	2200	–
Young's modulus – E (GPa)	75	25	–
Poisson's ratio – ν	0.2	0.2	–
Fracture Energy – G_c (J/m^2)	60	50	30
Tensile Strength – f_{ct} (MPa)	10	4	2.4 [1]
Cohesive zone length – l_z (mm)	41	72	–

The relationship between the cohesive element law and G_c introduces a length scale – called the cohesive zone length l_z – into the material description. This length has an important influence around the crack tip in numerical simulations and we shown that in our case it is of the order of 4 mm for the aggregates (see [29]). So the finite elements have to be smaller than 1 mm to have at least four elements in the cohesive zone.

4 The dynamic tensile response

As previously mentioned, the numerical model does not contain any random field to represent the scattering often observed on the macroscopic response of concrete. This scattering can be important in experimental tests for the same initial concrete mix but tested on several specimens. The main differences are then due to the different aggregate arrangements and to the macro-porosity distribution. In this section, we study only the influence of spatial distribution of aggregates and not the role of the macro-porosity. This porosity has probably a great influence on the crack initiation and ultimately on the crack path but in order to clearly separate the influence of aggregates, it will be omitted in our simulations.

The results of the strain-stress curves obtained for five numerical concrete specimens in tension for several strain rates are presented in Figure 4. One can see on this figure that the microstructure has a slight influence (less than 4 %) on the peak strength value of our concrete. The macroscopic tensile strength is mainly governed in our case by the ITZ strength and not by the meso-structure. This can be best explained by examining the failure process in quasi-static for which we can observe a gradual transition from diffuse micro-cracking to strain localization and finally to a macroscopic crack. Figure 5

[1] This value is estimated from G_c of the ITZ with δ_c equal to the value obtained for the mortar. With this assumption we obtain a f_{ct} smaller in the ITZ than in the mortar, which is commonly accepted for a classical concrete

shows this evolution to a unique macroscopic crack for $\dot{\varepsilon} = 0.1$ /s. In the upper row of Figure 5, which was obtained at the peak stress just before strain localization, one can remark that for the five meso-structures, the micro-cracks are diffuse and that their numbers are almost independent of the aggregates spatial distribution. This explains the slight influence on the peak strength value observed at the macroscopic scale. Conversely, on the lower row of Figure 5, which is extracted from the softening part, we notice that the crack path is strongly dependent on the meso-structure. This is why one obtains a stronger difference (50 %) on the stress value for $\varepsilon = 3.10^{-4}$ at the end of the loading for $\dot{\varepsilon} = 0.1$ /s.

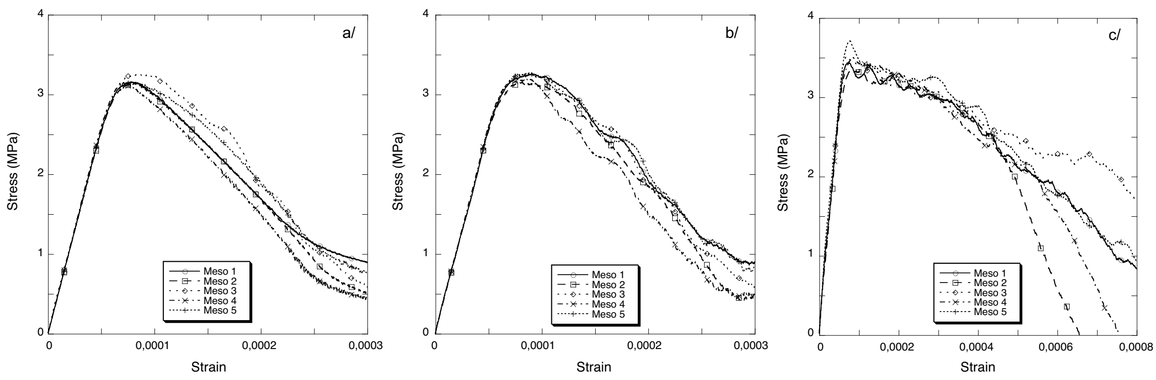

Figure 4: Influence of the meso-structure on the stress-strain curves for different strain rates: a/ $\dot{\varepsilon} = 0.1$ /s, b/ $\dot{\varepsilon} = 1$ /s, c/ $\dot{\varepsilon} = 10$ /s

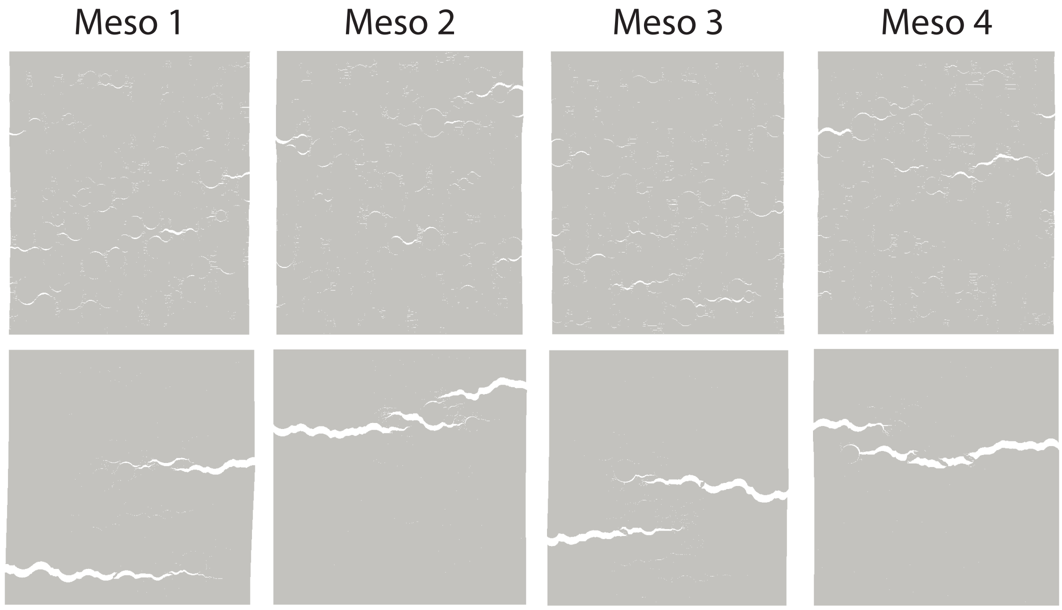

Figure 5: Influence of the meso-structure on the crack path for different meso-structures at $\dot{\varepsilon} = 0.1$ /s: upper row at $\varepsilon = 7.10^{-5}$ for $\approx$ the peak stress (disp. $\times$ 2000), lower row at $\varepsilon = 3.10^{-4}$ (disp. $\times$ 100)

5 Loading rate effect

It is well-known that experimental results on dynamic tension tests show a rate sensitivity of tensile strength [27, 12]. In quasi-statics, the macroscopic tensile strength is mainly governed in our case by the Interfacial Transition Zone strength (ITZ between the aggregates and the mortar paste) and not by the meso-structure [28, 29]. For low strain rate – $\dot{\varepsilon} < 1$ /s – the dynamic resistance increase is mainly due to the presence of water in the material [30] and we have a slight Dynamic Increase Factor – equal to the ratio of the static versus the dynamic strengths. For higher strain rate – $\dot{\varepsilon} > 1$ /s – the usual explanation of a more important DIF is the transition between single cracking in quasi-statics to diffuse cracks in dynamics.

The results of the strain-stress curves obtained for our numerical simulations in tension for several strain rates are presented in Figure 4. We can see on this figure the numerical rate effect in tension obtained. We can notice that in our case the dynamic increase factor is equal to almost 2 for $\dot{\varepsilon}$ = 100 /s which can be to slight compared to experimental one ($\sim$ 3). We may have to take into account rate dependency at the material level, for example by linking the cohesive strength f_{ct} to the rate of deformation of the surrounding material and to the crack opening rate, in order to achieve better agreement with experimental results.

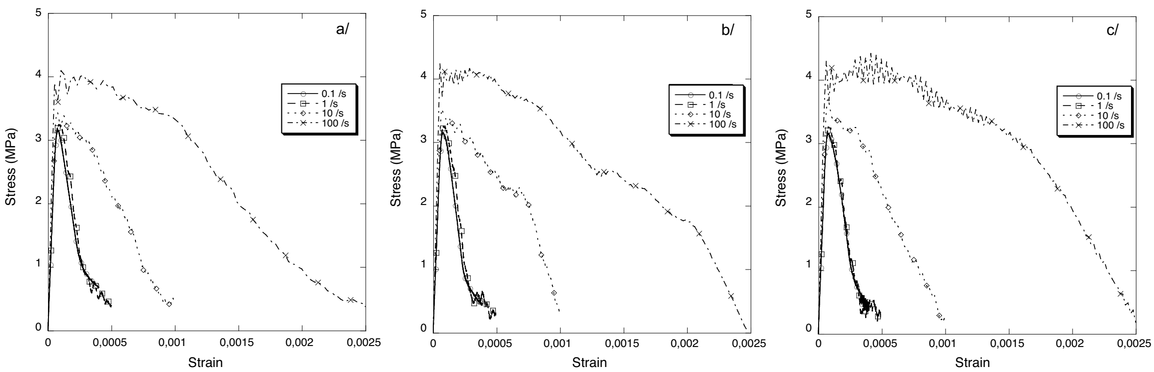

Figure 6: Numerical rate effect in tension for three meso-structures

Figure 6 shows the numerical rate effect in tension obtained for three meso-structures with our assumptions. One can see on this figure that the computed increase with strain rate is slight concerning the tensile strength. We obtain here a dynamic increase factor – equal to the ratio of the static versus the dynamic strengths – of 1.3 for $\dot{\varepsilon}$ = 100 /s while it is equal to approximately 3 in the experiments. This result shows that the assumption of no rate effect in the cohesive traction law is not totally realistic. The micro-inertia effects in the fracture process zone are not sufficient to explain the rate dependency of concrete in tension even at the highest loading rate velocities. One has to take into account a rate dependency at the material level, for example by linking the cohesive strength f_{ct} to the strain rate.

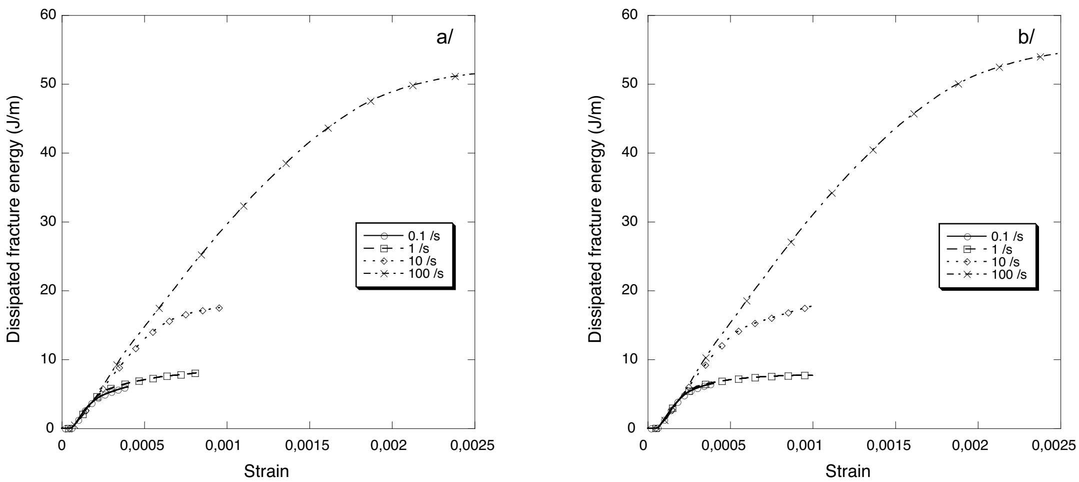

Figure 7: Influence of the meso-structure on the dissipated fracture energy for different strain rates

Figure 7 depicts the evolution of the dissipated fracture energy as a function of the macroscopic strain of the specimen for different loading rates and heterogeneities. One can see on this figure that the dissipated fracture energy strongly depends on the loading rate even with a rate independent local fracture energy. We note that even if the dynamic increase factor for the tensile strength is not large enough, it is less the case for the dissipated fracture energy of the specimen.

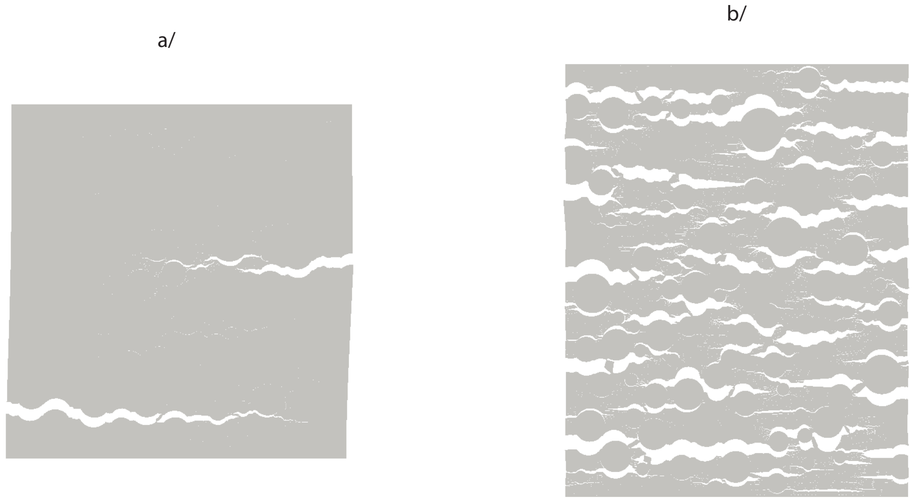

Figure 8: Influence of the loading rate on the final cracking for the meso-structure Meso 1 (disp. $\times$ 100): a/ $\dot{\varepsilon}$ = 0.1 /s, b/ $\dot{\varepsilon}$ = 100 /s,

According to the structural effect hypothesis, the explanation of higher dissipated fracture energy for high loading rates resides in a more diffuse micro-cracking. This effect can be seen on Figure 8 where the final aspect of the concrete specimen based on the meso-structure Meso 1 are compared for low and high loading rates. This behavior only explains that the differences between low and high loading rates are not important for the peak stress but only for the total dissipated fracture energy, which is in contradiction with experimental observations.

To improve our simulations and the representativeness of our numerical concrete, the challenge will be to find a rate dependent cohesive traction law (at least for the f_{ct} value) that will not increase too much the total dissipated fracture energy. But an open question remains. Should we use a rate dependent function for only the ITZ, mortar, or aggregates or for all the parts of the meso-structure? This point will be difficult to answer without some specific experiments on the different constituents of a real concrete.

6 Conclusion

In this paper we proposed a mesoscopic model for the analysis of dynamic tensile failure of concrete. This model is based on a 2D finite element description with cohesive capability of a mix of aggregates larger than 4 mm in a mortar paste matrix. The influence of the heterogeneous meso-structure of concrete and the loading rate on the tensile response and the dissipated fracture energy are studied. With our specimen size we observe a small impact of the aggregates arrangement on the tensile strength. This is of course based on the strong assumption of a perfect mix with no macro-porosity. Nevertheless when the post-peak response and then the dissipated fracture energy are considered, we show that the meso-structure has an influence.

The second main interest of the paper is the study of the dynamic loading rate effects on the tensile strength and on the dissipated fracture energy with our approach. The cohesive law used is independent of the local or global strain rate to see if the dynamic increase factor observed experimentally is due to a material effect or a structural (inertial) effect. The conclusions are not the same for the tensile strength and for the dissipated fracture energy. In the first case, the numerical results exhibit a small rate effect that is not coherent with the experiments. One the other hand, it is very interesting to see that for the second case we are very close to the experimental results. This means that the tensile strength increase is mostly due to a material effect (moisture, visco-elasticity, ...) while the dissipated fracture energy observed in the post-peak part is more due to the increase of the number of microcracks with the loading rate. With a small change in the cohesive law it will then be possible to have a realistic virtual material to test the influence of other experimental configurations.

References

[1] N.S. Ottosen. Constitutive model for short-time loading of concrete. *Journal of the Engineering Mechanics Division-ASCE*, 105(1):127–141, 1979.

[2] L.J. Sluys. *Wave propagation, localisation and dispersion in softening solids*. Doct. Dissertation, Delft University of Technologie–Delft, 1992.

[3] JF Dubé, G Pijaudier-Cabot, and C La Borderie. Rate dependent damage model for concrete in dynamics. *Journal of Engineering Mechanics-ASCE*, 122(10):939–947, 1996.

[4] J Sercombe, FJ Ulm, and F Toutlemonde. Viscous hardening plasticity for concrete in high-rate dynamics. *Journal of Engineering Mechanics-ASCE*, 124(9):1050–1057, 1998.

[5] ZP Bazant, FC Caner, MD Adley, and SA Akers. Fracturing rate effect and creep in microplane model for dynamics. *Journal of Engineering Mechanics-ASCE*, 126(9):962–970, 2000.

[6] F. Gatuingt and G. Pijaudier-Cabot. Coupled damage and plasticity modelling in transient dynamic analysis of concrete. *Int. J. Numer. Anal. Meth. Geomec.*, 26:1–24, 2002.

[7] G Hervé, F Gatuingt, and A Ibrahimbegovic. On numerical implementation of a coupled rate dependent damage-plasticity constitutive model for concrete in application to high-rate dynamics. *Engineering Computations*, 22(5-6):583–604, 2005.

[8] R.R. Pedersen, A. Simone, and L.J. Sluys. An analysis of dynamic fracture in concrete with a continuum visco-elastic visco-plastic damage model. *Engineering Fracture Mechanics*, 75:3782–805, 2008.

[9] F. Gatuingt, R. Desmorat, M. Chambart, D. Combescure, and D. Guilbaud. Anisotropic 3d delay-damage model to stimulate concrete structures. *Revue Européenne de mécanique numérique*, 17:740–60, 2008.

[10] Christophe Pontiroli, Alain Rouquand, and Jacky Mazars. Predicting concrete behaviour from quasi-static loading to hypervelocity impact An overview of the PRM model. *European Journal of Environmental and Civil Engineering*, 14(6-7):703–727, 2010.

[11] J. Weerheijm, I. Vegt, and K. van Breugel. The rate dependency of concrete in tension - New data for wet, normal and dry conditions. In *DYMAT 2009: 9th Inter. Conf. on the Mechanical and Physical Behaviour of Material under Dynamic Loading, Vol. 1*, pages 95–101, 2009.

[12] B. Erzar and P. Forquin. An Experimental Method to Determine the Tensile Strength of Concrete at High Rates of Strain. *Experimental Mechanics*, 50(7):941–955, 2010.

[13] S. Levy, J. F. Molinari, I. Vicari, and A. C. Davison. Dynamic fragmentation of a ring: Predictable fragment mass distributions. *Phys. Rev. E*, 82(6, Part 2), 2010.

[14] L. Snozzi, A. Caballero, and J.F Molinari. Influence of the meso-structure in dynamic fracture simulation of concrete under tensile loading. *Cement and Concrete Research*, 41:1130–1142, 2011.

[15] P. Roelfstra, H. Sadouki, and F. Wittmann. Le béton numerique. *Materials & Structures - RILEM*, 18:309–317, 1985.

[16] T. Stankowski. *Numerical simulation of progressive failure in particle composites.* PhD thesis, University of Colorado, USA, 1990.

[17] C Lopez. *Microstructural analysis of concrete fracture using interface elements. Application to various concretes.* PhD thesis, Universitat PolitÃ¨cnica de Catalunya, Spain, 1999.

[18] A. Caballero. *3D meso-mechanical numerical analysis of concrete using interface elements.* PhD thesis, Universitat PolitÃ¨cnica de Catalunya, Spain, 2005.

[19] T.D. N'Guyen, C. Lawrence, C. La Borderie, and G. Nahas. A mesoscopic approach for a better understanding of the transition from diffuse damage to localized damage. *European Journal of Environmental and Civil Engineering*, 14:751–776, 2010.

[20] L.A. Langer, W.C. Carter, and E.R. Fuller. The ppm2oof manual. Technical report, NIST, 2009.

[21] A. Hillerborg, E. Modéer, and P.E. Petersson. Analysis of crack formation and crack growth in concrete by means of fracture mechanics and finite elements. *Cement and Concrete Research*, 6(6):773–781, 1976.

[22] G.T. Camacho and M. Ortiz. Computational modelling of impact damage in brittle materials. *International Journal of Solids and Structures*, 33(20-22):2899–2938, 1996.

[23] I. Carol, C.M. Lopez, and O. Roa. Micromechanical analysis of quasi-brittle materials using fracture-based interface elements. *International Journal for numerical methods in enginnering*, 52(1-2):193–215, 2001.

[24] D.S Dugdale. Yielding of steel sheets containing slits. *Journal of the Mechanics and Physics of Solids*, 8:100–108, 1960.

[25] G.I. Barenblatt. The mathematical theory of equilibrium of cracks in brittle fracture. *Advances in Applied Mechanics*, 7:55–129, 1962.

[26] O. Miller, L.B. Freund, and A. Needleman. Modeling and simulation of dynamic fragmentation in brittle materials. *International Journal of Fracture*, 96(2):101–125, 1999.

[27] I Vegt, Pedersen R.R., Sluys L.J., and J. Weerheijm. Modelling of impact behaviour of concrete - an experimental approach. In *Computational Modelling of Concrete Structures - EURO-C 2006*, pages 451–458, 2006.

[28] RR Pedersen, A Simone, M Stroeven, and L.J. Sluys. Mesoscopic modelling of concrete under impact. In *6th International Conference on Fracture Mechanics of Concrete and Concrete Structures - FRAMCOS VI*, pages 571–578, 2007.

[29] F. Gatuingt, L. Snozzi, and J.F. Molinari. Numerical determination of the tensile response and the dissipated fracture energy of concrete: role of the meso-structure and influence of the loading rate. *International Journal for Numerical and Analytical Methods in Geomechanics, accepted*.

[30] P. Rossi, J.G.M. van Mier, C. Boulay, and F. Le Maou. The dynamic behaviour of concrete: influence of free water. *Materials and Structures*, 25:509–514, 1992.